Complex magnetoelastic properties in the frustrated kagome-staircase compounds $(Co_{1-x}Ni_x)_3V_2O_8$

Q. Zhang,[1] W. Knafo,[1,2,3] P. Adelmann,[1] P. Schweiss,[1] K. Grube,[1] N. Qureshi,[4,5,6] Th. Wolf,[1]
H. v. Löhneysen,[1,2] and C. Meingast[1]

[1]*Institut für Festkörperphysik, Karlsruher Institut für Technologie, DE-76021 Karlsruhe, Germany*
[2]*Physikalisches Institut, Karlsruher Institut für Technologie, DE-76128 Karlsruhe, Germany*
[3]*Laboratoire National des Champs Magnétiques Intenses, UPR 3228, CNRS-UJF-UPS-INSA, 143 Avenue de Rangueil, FR-31400 Toulouse, France*
[4]*Institute for Materials Science, University of Technology, DE-64728 Darmstadt, Germany*
[5]*Institute Max von Laue-Paul Langevin, FR-38042 Grenoble Cedex 9, France*
[6]*II. Physikalisches Institut, Universität zu Köln, Zülpicherstr. 77, DE-50937 Köln, Germany*

(Received 12 July 2011; revised manuscript received 11 November 2011; published 28 November 2011)

High-resolution heat-capacity and thermal-expansion measurements on single crystals of the kagome-staircase compounds $(Co_{1-x}Ni_x)_3V_2O_8$ are presented. The parent compounds $Co_3V_2O_8$ and $Ni_3V_2O_8$ undergo a sequence of first- and second-order magnetic phase transitions. The low-temperature ($T \leqslant 40$ K) magnetic entropy evolves monotonically with the doping content x from the full value expected for Ni^{2+} $S = 1$ magnetic moments in $Ni_3V_2O_8$ to only half the value expected for Co^{2+} $S = 3/2$ moments in $Co_3V_2O_8$. The thermal-expansion coefficients α_i ($i = a$, b, and c) show a strong anisotropy for all $(Co_{1-x}Ni_x)_3V_2O_8$ compounds. The low-temperature expansivities indicate that Co doping (Ni doping) yields changes similar to uniaxial pressures along a or b (c). Linear Grüneisen parameters Γ_i are extracted for the three main axes i and are found to exhibit a complex temperature and doping dependence. For each axis, Γ_i and α_i exhibit a sign change at low temperature at the critical concentration $x_c \simeq 0.25$ where the incommensurate magnetic propagation vector changes. Our study motivates further investigations to understand how the multiple and complex parameters such as magnetic frustration, magnetic anisotropy, and mixture of $S = 1$ and $3/2$ ions affect the rich magnetoelastic properties of $(Co_{1-x}Ni_x)_3V_2O_8$.

DOI: 10.1103/PhysRevB.84.184429 PACS number(s): 75.30.Kz, 75.50.Ee, 65.40.−b

I. INTRODUCTION

The study of the kagome-staircase compounds $Co_3V_2O_8$ and $Ni_3V_2O_8$, which have the same orthorhombic ($Cmce$) crystal structure,[1] has recently stimulated a great deal of experimental and theoretical work. In these systems, two-dimensional geometrically frustrated magnetism results from a kagome-staircase arrangement perpendicular to the b axis of the magnetic ions. The magnetic lattice is composed of Co^{2+} $S = 3/2$ ions in $Co_3V_2O_8$ and Ni^{2+} $S = 1$ ions in $Ni_3V_2O_8$, with two nonequivalent magnetic sites.[2] For both compounds, a cascade of magnetic transitions at low temperatures has been reported,[3,4] which indicates competing magnetic interactions. Both systems are characterized by "high-temperature" incommensurate (HTI) magnetic order [below $T_{HTI,1} = 11.3$ K in $Co_3V_2O_8$ (Ref. 3) and below $T_{HTI,2} = 9.1$ K in $Ni_3V_2O_8$ (Ref. 4)] and by a low-temperature weakly ferromagnetic phase [below $T_{FM} = 6.2$ K in $Co_3V_2O_8$ (Ref. 3) and a canted antiferromagnetic phase below $T_{C'} = 2.2$ K in $Ni_3V_2O_8$ Ref. 4)]. Both systems have the same magnetic easy axis **a**. Interest in these systems arose with the discovery of a multiferroic regime in $Ni_3V_2O_8$ for $T_C = 3.9$ K$< T < T_{LTI,2} =$ 6.3 K, where canted antiferromagnetism is accompanied by a ferroelectric polarization.[5] Contrary to $Ni_3V_2O_8$, $Co_3V_2O_8$ is not multiferroic.[6] Recent neutron-scattering[7,8] and specific-heat[9] studies yielded the doping-temperature magnetic phase diagram of the substitutional compounds $(Co_{1-x}Ni_x)_3V_2O_8$ and the evolution of the magnetic structure of the system from $Co_3V_2O_8$ to $Ni_3V_2O_8$. From these measurements, only a single transition was reported for samples with nickel concentration $0.14 \leqslant x \leqslant 0.73$. A change of the magnetic structure was found to occur around $x_c = 0.25$ where the transition temperature $T_{HTI} \simeq 5.5$ K is the lowest.[8]

Here, we present a comprehensive study of the specific heat and thermal expansion of single-crystalline $(Co_{1-x}Ni_x)_3V_2O_8$ with $x = 0$, 0.12, 0.2, 0.28, 0.35, 0.5, and 1. We find the same sequence of transitions as reported in the literature[2–4,6,10–12] for the parent compounds $Co_3V_2O_8$ and $Ni_3V_2O_8$. The high resolution of our specific-heat and thermal-expansion experiments allows studying the temperature and doping evolution of these transitions and to derive a detailed temperature-doping phase diagram. Further, the magnetic Grüneisen parameters, which provide a sensitive probe of the volume and pressure dependences of the magnetic energy scales, can be derived from the combination of thermal-expansion and heat-capacity data. We will demonstrate that the behavior of the Grüneisen parameters in this system is complex, probably due to the presence of several competing magnetic energy scales. Parallels to the novel behavior expected at quantum phase transitions[13] will be discussed in detail. This paper is organized as follows. In Sec. II, we provide experimental details. In Sec. III, we present the specific-heat and thermal-expansion data, the derived uniaxial Grüneisen parameters, and, in addition, the magnetic phase diagram and the pressure dependences of the magnetic ordering temperatures. A short discussion is presented in Sec. IV. Finally, main conclusions from our work are drawn in Sec. V.

II. EXPERIMENTAL DETAILS

$(Co_{1-x}Ni_x)_3V_2O_8$ single crystals with Ni concentrations $x = 0$, 0.12, 0.2, 0.28, 0.35, and 0.5 were grown from fluxes

composed of Co_3O_4, NiO, and V_2O_5. $Ni_3V_2O_8$ single crystals were grown from a flux composed of BaO, NiO, and V_2O_5. The Ni concentrations x were determined assuming the validity of Vegard's law, i.e., a linear dependence of the lattice constants (measured using x-ray powder diffraction) on x. The crystals were cut to typical dimensions of about $5 \times 5 \times 2$ mm^3. The specific heat was measured using a physical properties measurement system (PPMS) from Quantum Design; a ^{3}He insert was used to reach the lowest temperature of 0.3 K. Since the standard PPMS software is not adapted to the study of sharp phase transitions, a relaxation method similar to the ones proposed in Refs. 14 and 15 was used to obtain reliable data close to first- and second-order phase transitions. The linear thermal expansion was measured between 2 and 300 K using a homemade high-resolution capacitance dilatometer[16,17] with heating and cooling rates of 6 or 20 mK/s, with a resolution $\Delta L/L = 10^{-8}$. For all samples, the thermal expansion was measured along the three main crystallographic directions **a**, **b**, and **c**.

III. RESULTS

A. Specific heat

The specific heat C_p of $Co_3V_2O_8$, $(Co_{0.5}Ni_{0.5})_3V_2O_8$, and $Ni_3V_2O_8$ is presented in Fig. 1 for $0.3 < T < 30$ K on a log-log scale. The same sequence of transitions as reported in the literature[2–4,6] is observed for the two parent compounds. Huge first-order anomalies are obtained at $T_{FM} = 6.00 \pm 0.05$ K in $Co_3V_2O_8$ and $T_C = 3.90 \pm 0.05$ K in $Ni_3V_2O_8$, where C_p reaches 285 Jmol^{-1}K^{-1} and 64 Jmol^{-1}K^{-1}, respectively (the peak heights are almost an order of magnitude higher than those reported in Refs. 2–4 and 6). The high quality of our single crystals and an appropriate procedure to analyze the data (relaxation method[14,15]) permitted this very high resolution. $(Co_{0.5}Ni_{0.5})_3V_2O_8$ exhibits a single second-order phase transition at 7.45 ± 0.50 K only (see Appendix). The specific heat $C_p(T)$ follows a T^3 dependence below 1.5 K in $Ni_3V_2O_8$ and a T^4 dependence for $2 < T < 4$ K in $Co_3V_2O_8$, leveling off below 2 K. These power-law dependences presumably result from low-energy magnetic excitations. The

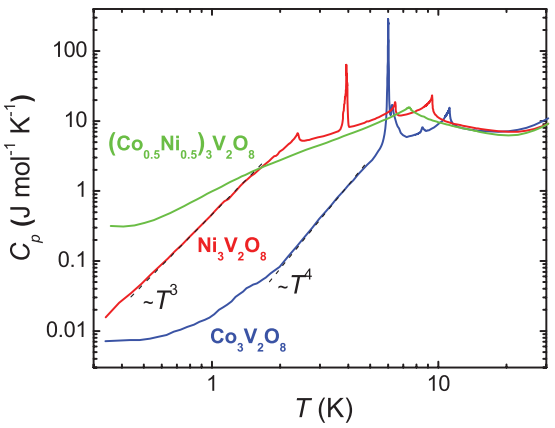

FIG. 1. (Color online) Specific heat C_p of $Co_3V_2O_8$, $(Co_{0.5}Ni_{0.5})_3V_2O_8$, and $Ni_3V_2O_8$ as a function of temperature T on a log-log scale. Dotted lines indicate the low-temperature T^3 and T^4 power-law regimes.

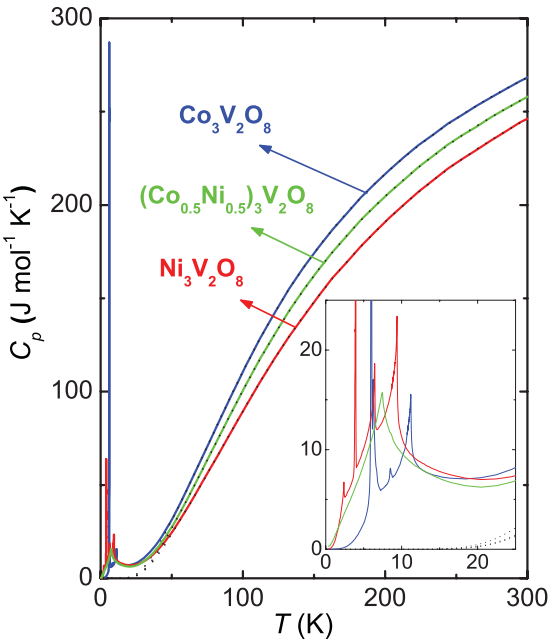

FIG. 2. (Color online) Specific heat C_p versus temperature T of $Co_3V_2O_8$, $(Co_{0.5}Ni_{0.5})_3V_2O_8$, and $Ni_3V_2O_8$. Dotted lines indicate a fit to the data above 60 K to obtain the phonon contribution to C_p (see text for details).

T^3 law in $Ni_3V_2O_8$ is compatible with three-dimensional ungapped antiferromagnetic spin waves arising in the canted antiferromagnetic state, which sets in below $T_C' \simeq 2$ K. The T^4 behavior in $Co_3V_2O_8$ might result from more complex spin dynamics.[18] Gapped spin waves have been reported by inelastic neutron scattering for $Co_3V_2O_8$ (Ref. 19) and the question is whether they could explain (or not) our low-temperature specific-heat data. The cascades of magnetic transitions in $Co_3V_2O_8$ and $Ni_3V_2O_8$ are accompanied by an additional signal proportional to T. For the intermediate $(Co_{0.5}Ni_{0.5})_3V_2O_8$ compound, the low-temperature specific heat is enhanced, indicating stronger low-energy magnetic excitations than those present in the parent compounds.

Figure 2 shows a plot of C_p versus T up to 300 K for $Co_3V_2O_8$, $(Co_{0.5}Ni_{0.5})_3V_2O_8$, and $Ni_3V_2O_8$, together with estimates of the phonon background. This nonmagnetic background was modeled by a combination of one Debye and two Einstein phonon modes, which were fitted to describe the data above 60 K (assuming that here the signal is due to the lattice). The phonon backgrounds extrapolated to lower T were subtracted from the measured specific heat to obtain the magnetic heat capacity C_{mag} shown in Fig. 3(a) as C_{mag}/T versus T for $0.3 < T < 60$ K, for $(Co_{1-x}Ni_x)_3V_2O_8$ samples with $x = 0$, 0.12, 0.2, 0.28, 0.35, 0.5, and 1. From our specific-heat data, we infer that $Co_3V_2O_8$ undergoes the series of transitions $T_{HTI,1} = 11.26 \pm 0.02$ K (high-temperature incommensurate phase), $T_{HTC,1} = 8.50 \pm 0.05$ K (high-temperature commensurate phase), $T_{LTI,2} = 6.20 \pm 0.05$ K (low-temperature incommensurate phase), and $T_{FM} = 6.00 \pm 0.05$ K (low-temperature ferromagnetic phase), while $Ni_3V_2O_8$ is characterized by the transitions $T_{HTI,2} = 9.42 \pm 0.02$ K (high-temperature incommensurate phase), $T_{LTI,2} = 6.48 \pm 0.02$ K (low-temperature incommen-

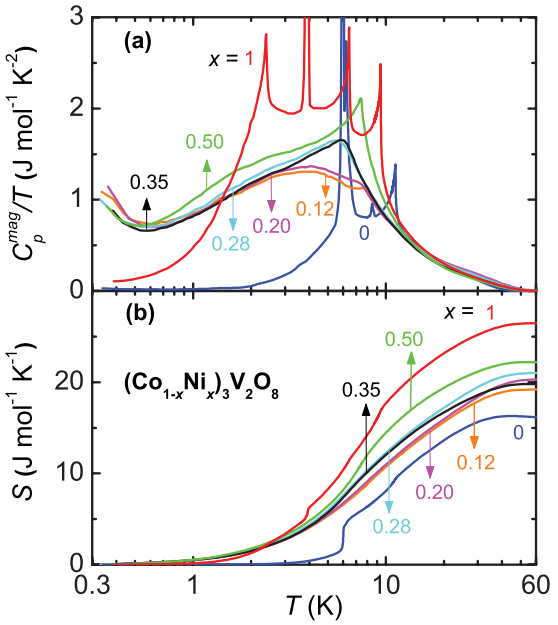

FIG. 3. (Color online) (a) Magnetic specific heat divided by temperature C_p^{mag}/T versus T. (b) Magnetic entropy S versus temperature T of $(\mathrm{Co}_{1-x}\mathrm{Ni}_x)_3\mathrm{V}_2\mathrm{O}_8$ single crystals.

surate phase), $T_{C,2} = 3.93 \pm 0.02$ K (canted antiferromagnetic phase), and $T_{C',2} = 2.42 \pm 0.03$ K (second canted antiferromagnetic phase) (see Appendix). The transitions at $T_{\mathrm{HTC},1}$, $T_{\mathrm{LTI},2}$, and T_{FM} in $\mathrm{Co_3V_2O_8}$, as well as at $T_{C,2}$ in $\mathrm{Ni_3V_2O_8}$ are first-order [steplike anomaly in $S_{\mathrm{mag}}(T)$, see below]. In contrast to the parent compounds, the heat capacities of the crystals with $x = 0.12$, 0.2, 0.28, 0.35, and 0.5 show only one phase transition, which is of second order, at 8.19 ± 0.10 K, 7.6 ± 0.2 K, 6.4 ± 0.4 K, 7.0 ± 0.4 K, and 7.9 ± 0.3 K, respectively. The transition temperature passes a minimum at $x = 0.28$. For the intermediate compositions, C_p^{mag}/T increases with decreasing temperature below 0.5 K.

The magnetic entropy S_{mag} obtained by integrating C_p^{mag}/T versus T is shown for different x in Fig. 3(b). Clear steplike increases of the magnetic entropy are observed at the first-order transitions T_{FM} in $\mathrm{Co_3V_2O_8}$ and $T_{C,2}$ in $\mathrm{Ni_3V_2O_8}$. In Fig. 4, the magnetic entropy acquired at 40 K [from Fig. 3(b)] is plotted as a function of x. For $\mathrm{Ni_3V_2O_8}$, S_{mag} at 40 K is equal to the full entropy $3R\ln 3$ from $\mathrm{Ni^{2+}}$ ions with $S = 1$, as already reported in Refs. 2 and 4. For $\mathrm{Co_3V_2O_8}$, S_{mag} reaches at 40 K only half of the full entropy $3R\ln 4$ expected for the $\mathrm{Co^{2+}}$ ions with $S = 3/2$, again in accordance with previous studies.[2,6] Rogado *et al.*[2] initially proposed that the missing entropy could be related to additional magnetic transitions occurring below 4 K (4 K was the lowest temperature investigated in their study). However, Fig. 3(a) shows that the magnetic specific heat of $\mathrm{Co_3V_2O_8}$ decreases strongly with decreasing temperature down to 0.3 K, with no indication whatsoever of a further transition below 0.3 K. Alternatively, Yasui *et al.*[6] proposed that the crystal-field splitting of the $S = 3/2$ quadruplet leads to a ground state of an effective $S_{\mathrm{eff}} = 1/2$ doublet, with a total magnetic entropy of $3R\ln 2$, i.e., half of $3R\ln 4$. The hypothesis of a larger crystal-field splitting in $\mathrm{Co_3V_2O_8}$ than in $\mathrm{Ni_3V_2O_8}$ is compatible with susceptibility measurements,[20–22] which showed that the magnetic properties of $\mathrm{Co_3V_2O_8}$ are very

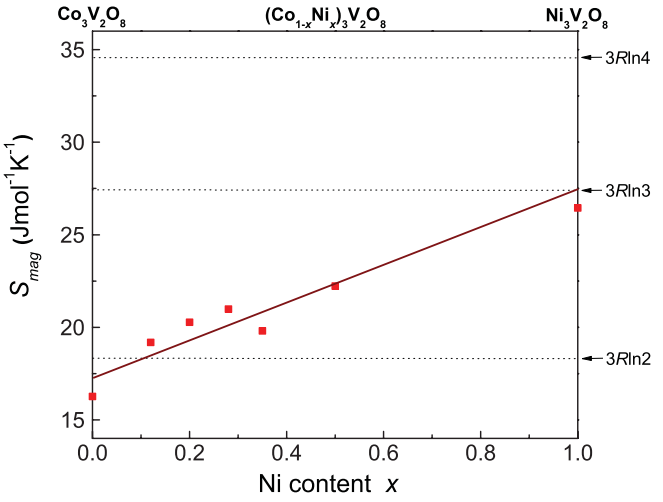

FIG. 4. (Color online) Magnetic entropy S_{mag} of $(\mathrm{Co}_{1-x}\mathrm{Ni}_x)_3\mathrm{V}_2\mathrm{O}_8$, at $T = 40$ K, as a function of the Ni concentration x.

anisotropic, while those of $\mathrm{Ni_3V_2O_8}$ are almost isotropic. We note that a similar situation occurs in the chlorides $\mathrm{CoCl_2}$ and $\mathrm{NiCl_2}$, where crystal-field effects are stronger in $\mathrm{CoCl_2}$ than in $\mathrm{NiCl_2}$.[23]

B. Thermal expansion and Grüneisen parameters

Figures 5(a) and 5(b) show the temperature dependence of the thermal-expansion coefficients α_i ($i = a$, b, and c) of $\mathrm{Co_3V_2O_8}$ and $\mathrm{Ni_3V_2O_8}$, respectively, for $2 < T < 300$ K.

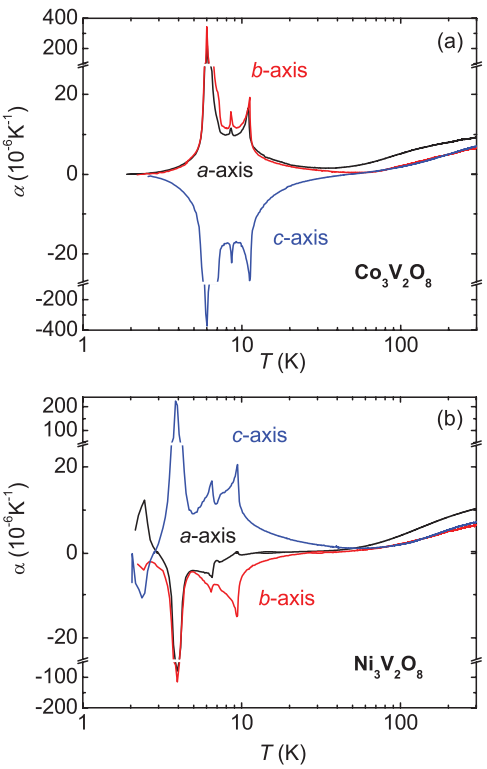

FIG. 5. (Color online) Thermal expansion coefficients α_a, α_b, and α_c versus temperature T of (a) $\mathrm{Co_3V_2O_8}$ and (b) $\mathrm{Ni_3V_2O_8}$.

They are defined as $\alpha_i = (1/L_i)\partial L_i/\partial T$, where L_i is the length along i. For both compounds, the thermal expansion shows the same sequences of phase transitions as the specific heat (Sec. II) (Table I, and Appendix). The thermal-expansion anomalies of $Co_3V_2O_8$ are positive and of roughly the same magnitude for the a and b axes, and negative for the c axis. Interestingly, this situation is reversed for $Ni_3V_2O_8$, which has essentially negative anomalies along the a and b axes and positive anomalies along the c axis. Above about 50 K, the magnetic contributions vanish and both compounds exhibit very similar expansion coefficients arising from lattice anharmonicities. For both compounds, α_b and α_c are nearly identical, while α_a is somewhat larger. The similarity of the phonon thermal expansion for both compounds (with the same crystal structure) is not unexpected since Co and Ni are neighbors in the periodic table.

The detailed temperature dependence of the thermal-expansion coefficients, the integrated relative length changes, and the uniaxial Grüneisen parameters for various Ni concentrations x are displayed in Fig. 6. We follow Ref. 13 in defining the uniaxial Grüneisen parameters Γ_i as simply the ratio α_i/C_p. The normalized lengths $[L_i - L_i(30\ \mathrm{K})/L_i(30\mathrm{K})]$ for $Co_3V_2O_8$ and $Ni_3V_2O_8$ and $i = a,b,c$ again nicely demonstrate the anisotropy discussed earlier and are in good agreement with previously reported values.[11,12] For the intermediate compounds, there is a progressive evolution from the Co-type anisotropic behavior to the Ni-type behavior as x increases. These compounds all exhibit only a single phase transition, which can be identified as the transition at the highest temperature of the parent compounds. Only the $x = 0.12$ sample does show two transitions. The anomalies in α_i are strongly reduced for the intermediate compounds. The change of behavior from Co- to Ni-like occurs around $x = 0.20$–0.28. At these concentrations, the behavior is quite peculiar; above T_{HTI}, α_i appears to behave Co-like, but at and below T_{HTI}, the α_i jump and sign change to Ni-like behavior. This is most apparent for the a- and c-axis data [cf. Figs. 6(d) and 6(f)]. We note that this jump occurs only in the thermal expansion and not in the heat capacity, where in the latter, the transition is visible as a kink only [cf. Fig. 3(a)]. Therefore, it is not at all apparent how one can apply the Ehrenfest relation to obtain the pressure dependences of T_{HTI}.

In order to reach a better understanding of the complex behavior described above, it is informative to examine the magnetic Grüneisen parameters Γ_i shown in Figs. 6(g) to 6(i). Despite the qualitative similarity to α_i, some important differences are noteworthy. We first discuss the behavior of Γ_i for the end compounds. The first remarkable observation is the complete absence of anomalies in Γ_a and Γ_c for $Co_3V_2O_8$ at both $T_{\mathrm{HTI},1}$ and $T_{\mathrm{HTC},1}$, and for $Ni_3V_2O_8$ at $T_{\mathrm{HTI},2}$. These Γ_i $(i = a,c)$ are not constant, their absolute values strongly increase as the temperature is reduced, peaking at the large first-order phase transition below which they decrease again. The behavior of Γ_b is similar, however, a sizable step is observed in Γ_b at $T_{\mathrm{HTI},1}$. Again, Γ_b of $Ni_3V_2O_8$ mirrors Γ_b of $Co_3V_2O_8$, with qualitatively very similar T dependence including a steplike feature at $T_{\mathrm{HTI},2}$. The absence of an anomaly in Γ_i $(i = a,c)$ at these phase transitions implies that the anomalies in α_i and C_p scale with a single parameter, which, however, is not constant, but rather increases with decreasing temperature, passes over a maximum around the low-temperature transitions, and then decreases again [see Figs. 6(g) to 6(i)].

The Grüneisen parameters probe the volume (or pressure) dependence of the magnetic energy scales. For the simplest magnetic phase transition, one expects only the exchange energy to depend on volume (or pressure), leading to a temperature-independent Grüneisen parameter. Clearly, our results show that the situation in $Co_3V_2O_8$ and $Ni_3V_2O_8$ is much more complex. The Grüneisen parameters for the

TABLE I. Values of the transition temperatures, orders of the transitions, and signs of the uniaxial pressure dependences along a, b, and c of the transition temperatures.

Ni content x	Transition temperature	T_x (K)	Order	Sign of $\partial T_x/\partial p_a$	Sign of $\partial T_x/\partial p_b$	Sign of $\partial T_x/\partial p_c$
0 ($Co_3V_2O_8$)	$T_{\mathrm{HTI},1}$	11.25 ± 0.10	Second	+	+	−
	$T_{\mathrm{HTC},1}$	8.55 ± 0.10	First	+	+	−
	$T_{\mathrm{LTI},1}$	6.2 ± 0.1	First			
	T_{FM}	6.00 ± 0.05	First	+	+	−
0.12	$T_{\mathrm{HTI},1}$	8.0 ± 0.3	Second	+	+	−
	T_L	5.0 ± 0.5	Second	+	+	−
0.20	$T_{\mathrm{HTI},1}$	7.0 ± 0.5	Second	+	+	−
0.28	$T_{\mathrm{HTI},2}$	6.0 ± 0.4	Second	−	−	+
0.35	$T_{\mathrm{HTI},2}$	6.3 ± 0.4	Second	−	−	+
0.50	$T_{\mathrm{HTI},2}$	7.5 ± 0.3	Second	−	−	+
	$T_{\mathrm{HTI},2}$	9.5 ± 0.1	Second	+	−	+
1 ($Ni_3V_2O_8$)	$T_{x,2}$	7.20 ± 0.05	Second	+	+	−
	$T_{\mathrm{LTI},2}$	6.5 ± 0.1	Second	−	−	+
	T_C	3.90 ± 0.05	First	−	−	+
	$T_{C'}$	2.45 ± 0.10	Second	+	−	−

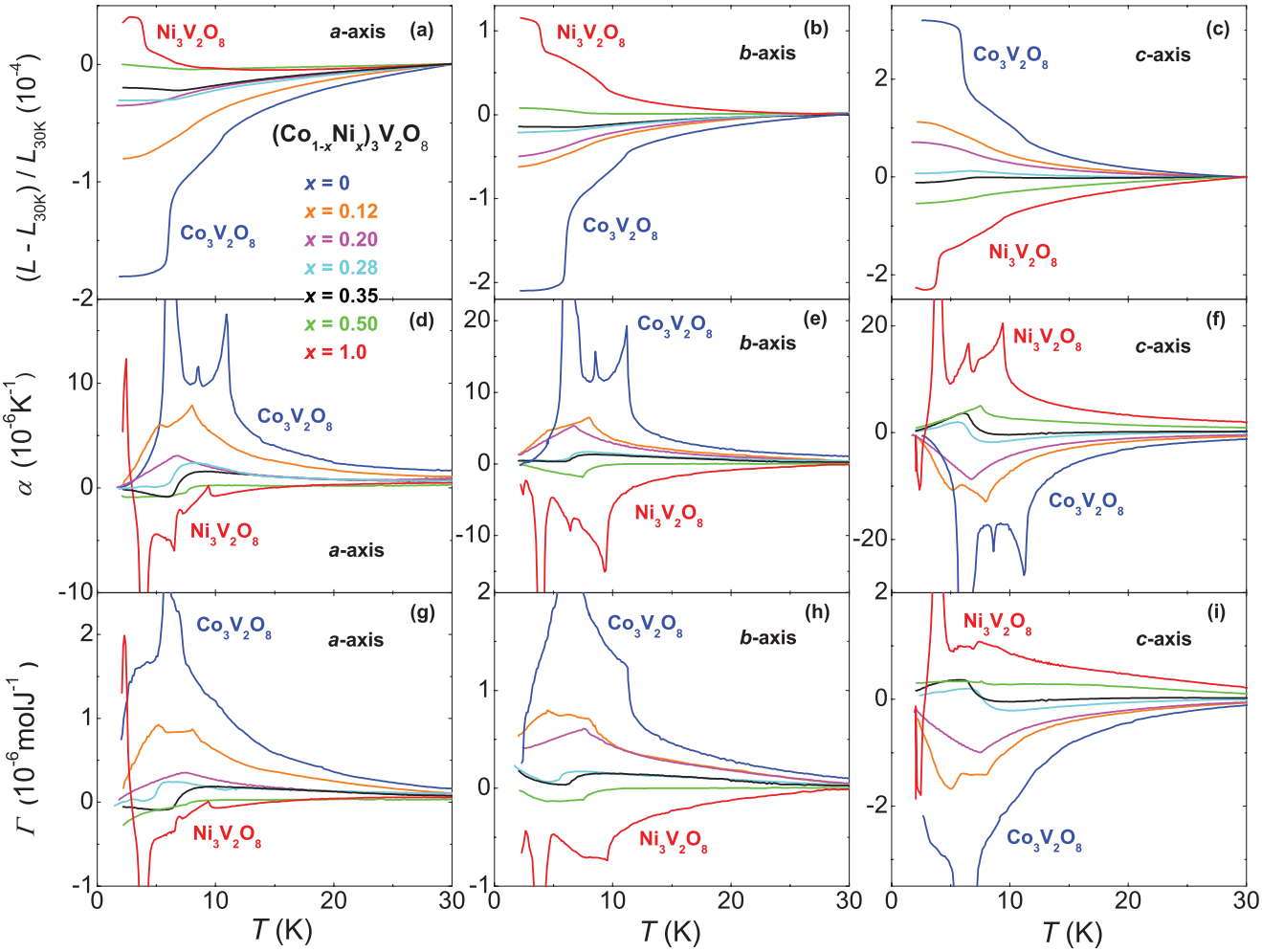

FIG. 6. (Color online) Temperature dependence of the relative length $[L(T) - L(30\text{K})]/\text{L}(30\text{ K})$ measured along the a, b, and c axes [(a), (b), and (c), respectively], of the thermal-expansion coefficient α extracted for the a, b, and c axes [(d), (e), and (f), respectively], and of the Grüneisen parameter Γ extracted for the a, b, and c axes [(g), (h), and (i), respectively] for $(Co_{1-x}Ni_x)_3V_2O_8$ samples of concentration $x = 0$, 0.12, 0.20, 0.28, 0.35, 0.5 and 1.

intermediate compounds evolve, like the α_i coefficients, from Co- to Ni-like behavior as the Ni content x increases. Two types of behavior are particularly interesting: they are shown in Fig. 7. For $x = 0.2$, Γ_i increases in absolute magnitude with decreasing T down to $T_{\text{HTI},1}$, which is visible as a sharp kink-like maximum in the curves. Below $T_{\text{HTI},1}$, the absolute magnitude of Γ_i decreases again sharply. This behavior is clearly different from that of pure $Co_3V_2O_8$ where the HTI,1 transition is hardly visible in Γ_i. For $x = 0.35$, on the other hand, all Γ_i exhibit a steplike change at $T_{\text{HTI},2}$, with a positive step, i.e., an increase of Γ_i with increasing T, for the a and b axes and a negative step for the c axis. All the above features point to a complex nature of magnetism in $(Co_{1-x}Ni_x)_3V_2O_8$, which will be discussed below.

C. Phase diagram and pressure dependences

Figure 8 presents the doping-temperature phase diagram of $(Co_{1-x}Ni_x)_3V_2O_8$ extracted from specific-heat and thermal-expansion data (see Sec. III and Appendix) and from neutron-scattering experiments.[8] The different data sets agree quite well with each other and indicate that T_{HTI} is minimal at a critical concentration $x_c \simeq 0.25$. The antiferromagnetic phase is denoted by HTI,1 for $x < x_c$ and HTI,2 for $x > x_c$, with the transition temperatures $T_{\text{HTI},1}$ and $T_{\text{HTI},2}$, respectively. These two phases are separated by a first-order transition at the critical concentration x_c, where the direction of the incommensurate propagation vector changes.[8] Changes of sign in the thermal-expansion coefficients and Grüneisen parameters are observed close to x_c.

The transition temperatures extracted for the compounds $(Co_{1-x}Ni_x)_3V_2O_8$, as well as their order and the sign of their uniaxial pressure dependences, are summarized in Table I (see also Appendix). Using the Clapeyron relation

$$\frac{\partial T_x}{\partial p_i} = \frac{\Delta L_i V}{\Delta S}, \tag{1}$$

where $\partial T_x/\partial p_i$ is the uniaxial pressure dependence of a first-order transition temperature T_x, ΔL_i and ΔS the length and entropy changes at the transition, respectively, p_i the uniaxial pressure applied along i, and V the molar volume, we calculate the uniaxial pressure dependences of $T_{\text{HTC},1}$ and T_{FM} in $Co_3V_2O_8$ and T_C in $Ni_3V_2O_8$ (see

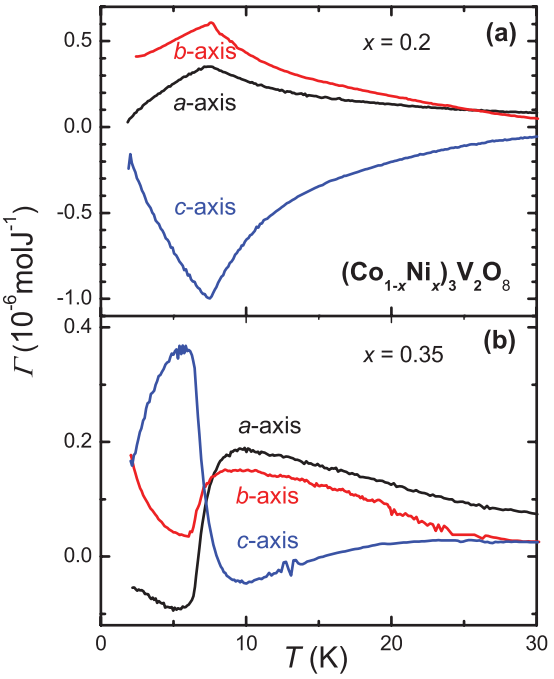

FIG. 7. (Color online) Temperature dependence of the Grüneisen parameters Γ_i on an expanded vertical scale of (a) $(Co_{0.8}Ni_{0.2})_3V_2O_8$ and (b) $(Co_{0.65}Ni_{0.35})_3V_2O_8$ for the a, b, and c axes.

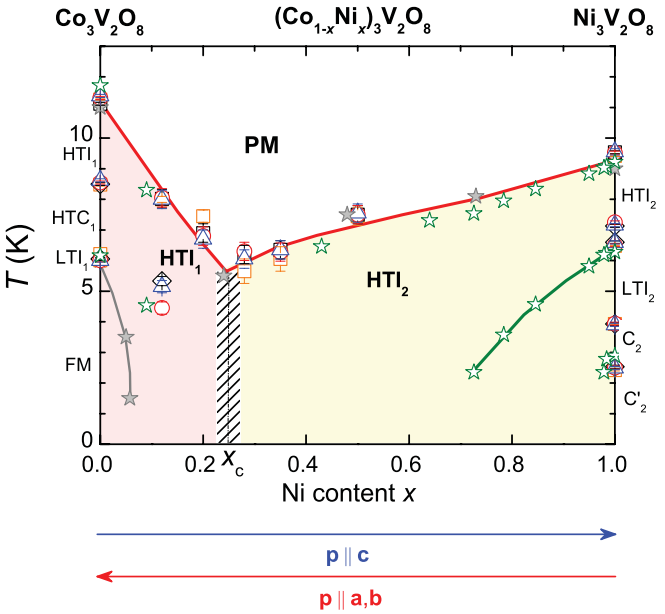

FIG. 8. (Color online) Magnetic (T,x) phase diagram of $(Co_{1-x}Ni_x)_3V_2O_8$ extracted from the specific heat (squares) and thermal expansion (diamonds: a axis; circles: b axis; and triangles: c axis). Full stars correspond to transition temperatures extracted from neutron experiments by Qureshi *et al.* (Refs. 7 and 8) and open stars to transitions obtained from specific heat by Kumarasiri and Lawes (Ref. 24).

Table II). We find that $\partial \ln T_C/\partial p_i \simeq -5\partial \ln T_{\mathrm{HTC},1}/\partial p_i \simeq -(5/2)\partial \ln T_{\mathrm{FM}}/\partial p_i$. The signs of these pressure dependences indicate that uniaxial pressure applied along a or b induces an increase of $T_{\mathrm{HTC},1}$ and T_{FM} and a decrease of T_C, while uniaxial pressure applied along c has the opposite effects. The uniaxial pressure dependences of a second-order transition temperature T_x can be extracted using the Ehrenfest relation

$$\frac{\partial T_x}{\partial p_i} = \frac{\Delta\alpha_i V T_x}{\Delta C_p}, \tag{2}$$

where $\Delta\alpha_i$ and ΔC_p are the thermal-expansion and specific-heat changes at the transition. Table III presents the pressure dependences extracted for the second-order transitions $T_{\mathrm{HTI},1}$ in $Co_3V_2O_8$ and $T_{\mathrm{HTI},2}$, $T_{\mathrm{LTI},2}$, and $T_{C'}$ in $Ni_3V_2O_8$. The pressure dependences of $T_{\mathrm{HTI},1}$ and $T_{\mathrm{LTI},2}$ have the same signs as those of the first-order transitions of the corresponding compounds. $T_{\mathrm{HTI},2}$, $T_{x,2}$, and $T_{C'}$ can be considered anomalous since their uniaxial pressure dependences have different signs from those of the first-order transition T_C.

The magnetic transitions in the intermediate compounds are not associated with well-defined steplike anomalies in S, L_i, C_p, or α_i. Their uniaxial pressure dependences, therefore, can not be determined, in contrast to the parent compounds. We will therefore limit the discussion to the signs of the uniaxial-pressure-dependences of T_{HTI} (summarized in Table I), which are given by the signs of the thermal-expansion anomalies at T_{HTI}. The trend indicated by the first-order transitions in the parent compounds is followed by the transitions of the doped compounds. Indeed, $\partial T_{\mathrm{HTI},1}/\partial p_a, \partial T_{\mathrm{HTI},1}/\partial p_a > 0$, and $\partial T_{\mathrm{HTI},1}/\partial p_c < 0$ on the Co-rich side ($x < x_c$), while $\partial T_{\mathrm{HTI},2}/\partial p_a, \partial T_{\mathrm{HTI},2}/\partial p_a < 0$, and $\partial T_{\mathrm{HTI},2}/\partial p_c > 0$ on the Ni-rich side ($x > x_c$). Since $T_{\mathrm{HTI},1}$ decreases with x while $T_{\mathrm{HTI},2}$ increases with x [cf. the phase diagram of $(Co_{1-x}Ni_x)_3V_2O_8$ in Fig. 8], to first approximation the effects of uniaxial pressure along c are similar to those of Ni doping, while the effects of a uniaxial pressure along a or b are equivalent to that of Co doping. This simple picture is compatible with the signs of most pressure dependences of the parent compounds, i.e., all the first- and second-order transitions of $Co_3V_2O_8$, and the

TABLE II. Steplike variations of the entropy ΔS and the relative lengths $\Delta L_a/L_a$, $\Delta L_b/L_b$, and $\Delta L_c/L_c$ at the first-order transition temperatures $T_{\mathrm{HTC},1}$ and T_{FM} in $Co_3V_2O_8$ and T_C in $Ni_3V_2O_8$, and uniaxial pressure dependences of these transitions extracted using the Clapeyron relation.

Ni content x	Transition temperature	ΔS (mJ/molK)	$\Delta L_a/L_a$ (10^{-4})	$\Delta L_b/L_b$ (10^{-4})	$\Delta L_c/L_c$ (10^{-4})	$\partial(\ln T_x)/\partial p_a$ (kbar^{-1})	$\partial(\ln T_x)/\partial p_b$ (kbar^{-1})	$\partial(\ln T_x)/\partial p_c$ (kbar^{-1})
0 ($Co_3V_2O_8$)	$T_{\mathrm{HTC},1}$	0.04 ± 0.01	0.004 ± 0.001	0.009 ± 0.002	-0.010 ± 0.002	0.11 ± 0.05	0.21 ± 0.10	-0.26 ± 0.11
	T_{FM}	3.19 ± 0.30	0.54 ± 0.07	0.80 ± 0.10	-1.13 ± 0.15	0.24 ± 0.05	0.36 ± 0.08	-0.51 ± 0.12
1 ($Ni_3V_2O_8$)	T_C	1.08 ± 0.10	-0.26 ± 0.03	-0.34 ± 0.04	0.705 ± 0.080	-0.51 ± 0.11	-0.67 ± 0.14	1.41 ± 0.29

TABLE III. Steplike variations of the specific heat divided by temperature $\Delta C_p/T$ and of the thermal expansion $\Delta\alpha_a$, $\Delta\alpha_b$, and $\Delta\alpha_c$ at the second-order transition temperatures $T_{\mathrm{HTI},1}$ in $Co_3V_2O_8$ and $T_{\mathrm{HTI},2}$, $T_{\mathrm{LTI},2}$, and $T_{C'}$ in $Ni_3V_2O_8$, and uniaxial pressure dependences of these transitions extracted using the Ehrenfest relation.

Ni content x	Transition temperature	$\Delta C_p/T_x$ (mJ/molK)	$\Delta\alpha_a$ (10^{-6} K^{-1})	$\Delta\alpha_b$ (10^{-6} K^{-1})	$\Delta\alpha_c$ (10^{-6} K^{-1})	$\partial(\ln T_x)/\partial p_a$ (10^{-2} kbar^{-1})	$\partial \ln T_x/\partial p_b$ (10^{-2} kbar^{-1})	$\partial \ln T_x/\partial p_c$ (10^{-2} kbar^{-1})
0 ($Co_3V_2O_8$)	$T_{\mathrm{HTI},1}$	480 ± 70	8.24 ± 0.50	12.8 ± 0.8	-12.9 ± 2.0	1.2 ± 0.2	1.6 ± 0.3	-1.6 ± 0.4
	$T_{\mathrm{HTI},2}$	1005 ± 100	1.3 ± 0.2	-9.1 ± 0.8	11.4 ± 1.0	0.12 ± 0.03	-0.8 ± 0.02	1.0 ± 0.2
1 ($Ni_3V_2O_8$)	$T_{\mathrm{LTI},2}$	1080 ± 100	-3.35 ± 0.50	-2.25 ± 0.25	6.49 ± 0.50	-0.4 ± 0.1	-0.300 ± 0.005	0.8 ± 0.1
	$T_{C'}$	881 ± 70	10 ± 1	-2.98 ± 0.40	-9.1 ± 1.0	3.8 ± 0.7	-1.1 ± 0.2	-3.5 ± 0.4

transitions $T_{\mathrm{LTI},2}$ and T_C in $Ni_3V_2O_8$. $T_{\mathrm{HTI},2}$, $T_{x,2}$, and $T_{C'}$ in $Ni_3V_2O_8$ are exceptions to the picture proposed here.

IV. DISCUSSION

While $Co_3V_2O_8$ and $Ni_3V_2O_8$ present complex sequences of low-temperature phase transitions, the magnetic phase diagram of $(Co_{1-x}Ni_x)_3V_2O_8$ is relatively simple since a single second-order magnetic phase transition (at $T_{\mathrm{HTI},1}$ or $T_{\mathrm{HTI},2}$) develops in the intermediate compounds of concentration $0.2 \leqslant x \leqslant 0.7$. However, as a function of doping, the temperature of this transition undergoes a discontinuous change of slope at $x_c \simeq 0.25$. Below $T_{\mathrm{HTI},1}$ or $T_{\mathrm{HTI},2}$, the transition at x_c is therefore presumably first-order since a discontinuous change of the magnetic wave vector[8] is involved. As in $Sr_3Ru_2O_7$ in a rotating magnetic field,[25] tuning an additional parameter (magnetic field, uniaxial pressure, etc.) might help to induce in $(Co_{1-x}Ni_x)_3V_2O_8$ a second-order critical endpoint at $T = 0$. Stronger magnetic fluctuations are expected at a second-order quantum phase transition, while a first-order transition usually yields a low-energy cutoff to quantum fluctuations. In the following, we will discuss briefly the scenario of $(Co_{1-x}Ni_x)_3V_2O_8$ being in the vicinity of a possible quantum phase transition near x_c. In heavy-fermion materials, magnetic quantum phase transitions have been studied in great detail,[26,27] and critical magnetic fluctuations[28,29] are known to enhance the low-temperature specific-heat,[30,31] thermal-expansion coefficients, and Grüneisen parameters[13,32] at the quantum phase transition. On the magnetic ordered side, a sign change of the low-temperature thermal-expansion coefficients and Grüneisen parameters has been predicted to occur at the (finite) transition temperature[13] and has been recently observed in the prototype heavy-fermion system $CeCu_{6-x}Au_x$.[33] In $(Co_{1-x}Ni_x)_3V_2O_8$, the sign change of the low-temperature thermal-expansion coefficients and Grüneisen parameters upon approaching x_c from the Ni-rich side, i.e., for $x = 0.2$ and 0.28 (see Figs. 6 and 7), is reminiscent of the proximity of a quantum phase transition. Interestingly, below x_c, α_i and Γ_i do not show a sign change but rather a cusplike extremum at the ordering temperature. This distinctly different behavior of α_i and Γ_i across x_c underlines the originality of $(Co_{1-x}Ni_x)_3V_2O_8$. Another interesting feature of the current system is the small size of the expansivity anomalies and associated Grüneisen parameters near x_c, both of which usually are largest at the critical point for a pressure-tuned system. Disorder may play a role here since the Grüneisen parameters show the smallest anomalies at $x = 0.5$, where disorder effects are expected to be maximal. In $Co_3V_2O_8$ and $Ni_3V_2O_8$, a high C_p/T background, in addition to the anomalies associated with the cascade of transitions (see Fig. 3), is presumably related to strongly fluctuating magnetic moments. A similar broad background in the specific heat was observed below T_N in the heavy-fermion prototypes $CeCu_{6-x}Au_x$ (Ref. 31) and $Ce_xLa_{1-x}Ru_2Si_2$ (Ref. 30). Magnetic fluctuations in $(Co_{1-x}Ni_x)_3V_2O_8$ might be a consequence of magnetic frustration. Quasielastic fluctuations observed up to at least 20 K in $Co_3V_2O_8$ (Ref. 19) recall those usually found in heavy-fermion materials. Upon doping, the low-temperature specific heat is enhanced close to x_c and is also possibly controlled by the spin fluctuations. It is interesting to note that the magnetic specific heat for $x = 0.28$ and 0.35 presents a cusplike behavior around $T_{\mathrm{HTI},2}$.

To understand the magnetic properties of $(Co_{1-x}Ni_x)_3V_2O_8$ in detail, a microscopic description of the magnetic interactions and of their uniaxial pressure dependences is needed as obtained, e.g., for $YTiO_3$ and $LaTiO_3$, where the uniaxial pressure dependences of T_C and T_N, respectively, were related to distortion-induced modifications of the superexchange.[34] However, the number of parameters is so large that solving the $(Co_{1-x}Ni_x)_3V_2O_8$ problem presents a major challenge. Both parent compounds exhibit a cascade of magnetic phases below 12 K with commensurate and incommensurate wave vectors, indicating the presence of a large number of magnetic interactions. Magnetic frustration and low dimensionality are key ingredients determining the magnetic properties of this family of compounds. The fact that $Ni_3V_2O_8$ is composed of $S = 1$ moments, while $Co_3V_2O_8$ is composed of $S = 3/2$ moments, affects of course the magnetic interactions and the magnetic single-ion anisotropy: this has to be considered in order to understand the properties of the parent compounds and of the intermediate compounds as well. Furthermore, the kagome-staircase lattice of the system consists of two inequivalent magnetic sites. Finally, a consequence of the complex magnetic properties, i.e., the presence of a multiferroic phase in $Ni_3V_2O_8$, has still an enigmatic origin and will certainly need considerable efforts before being understood.

V. CONCLUSION

In summary, we have examined in detail the magnetic phase transitions and phase diagram of $(Co_{1-x}Ni_x)_3V_2O_8$ using heat-capacity and high-resolution thermal-expansion measurements. For the parent compounds $Co_3V_2O_8$ and $Ni_3V_2O_8$, the sequences of transitions previously reported in

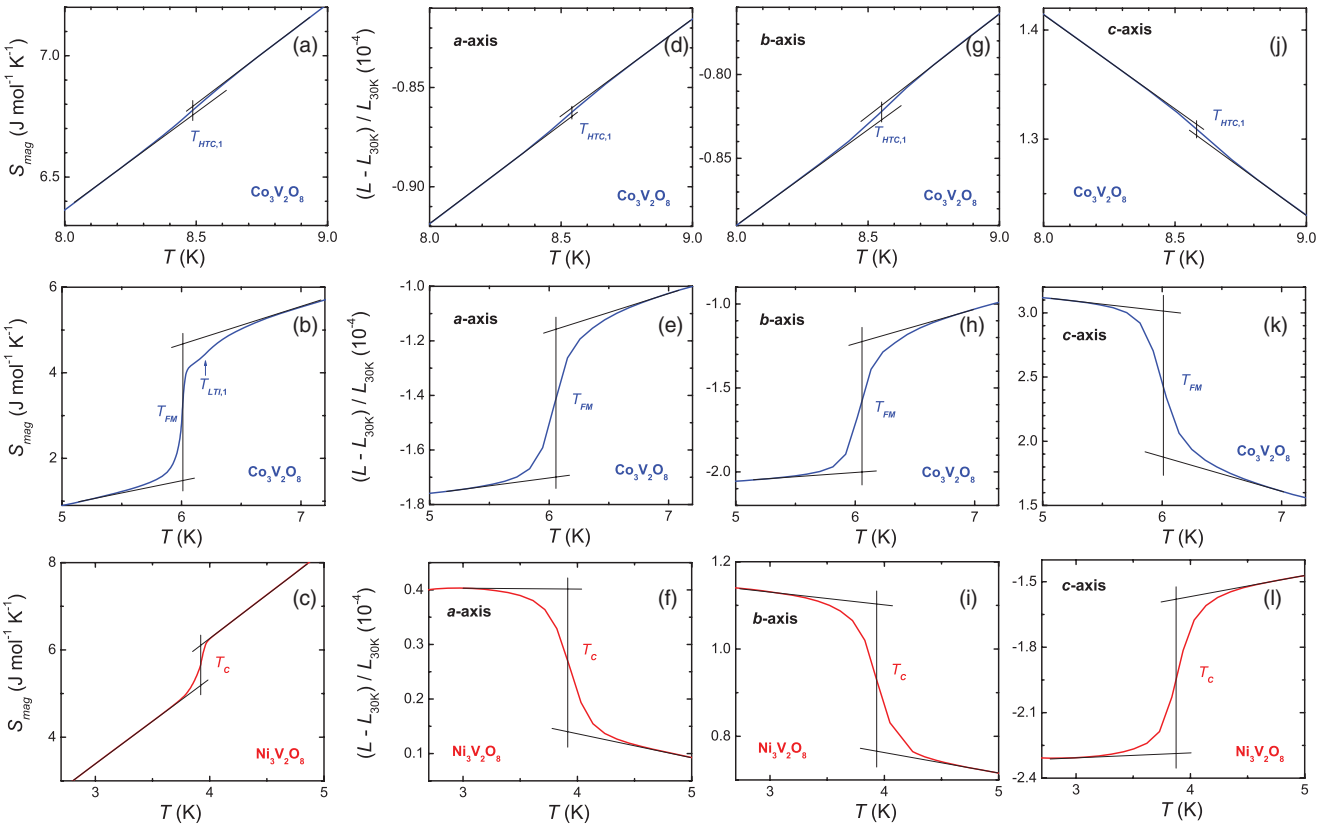

FIG. 9. (Color online) Anomalies in the magnetic entropy S_{mag} and length changes $\Delta L_i/L_i$ at the first-order transitions.

the literature are observed. Our heat-capacity data show that there are no further phase transitions down to 0.3 K. There is a smooth evolution of entropy upon substitution of Co by Ni from only half of the entropy expected for Co^{2+} $S = 3/2$ magnetic moments in $Co_3V_2O_8$ to the full entropy of Ni^{2+} $S = 1$ magnetic moments in $Ni_3V_2O_8$. The thermal-expansion data together with the heat-capacity data allow us to calculate the uniaxial pressure dependences of the transition temperatures without actually applying any real pressure. We find that the uniaxial pressure effects for both $Co_3V_2O_8$ and $Ni_3V_2O_8$ are extremely anisotropic along the three crystallographic directions. Intriguingly, the anisotropies of $Co_3V_2O_8$ and

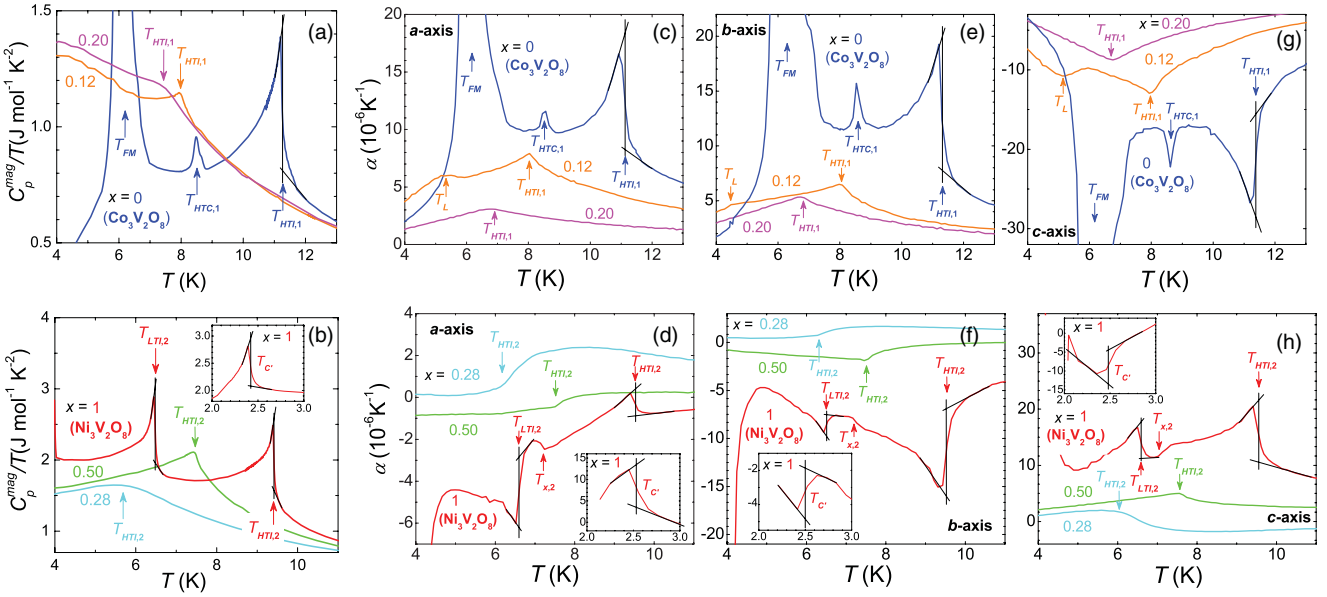

FIG. 10. (Color online) Anomalies of the magnetic specific heat divided by temperature C_p^{mag}/T and thermal-expansion coefficients α_i at the second-order transitions.

TABLE IV. Transition temperatures determined from our data (specific heat, thermal expansion along a, b, and c) and nature (first or second order) of the transitions.

Ni content x	Transition temperature	Order	From C_p (K)	From α_a (K)	From α_b (K)	From α_c (K)
	$T_{\mathrm{HTI},1}$	Second	11.26 ± 0.02	11.12 ± 0.05	11.31 ± 0.05	11.38 ± 0.05
0	$T_{\mathrm{HTC},1}$	First	8.50 ± 0.05	8.50 ± 0.05	8.55 ± 0.05	8.60 ± 0.05
($Co_3V_2O_8$)	$T_{\mathrm{LTI},1}$	First	6.21 ± 0.05			
	T_{FM}	First	6.01 ± 0.05	6.05 ± 0.05	6.01 ± 0.05	6.00 ± 0.05
0.12	$T_{\mathrm{HTI},1}$	Second	8.0 ± 0.1	8.0 ± 0.3	8.05 ± 0.30	8.0 ± 0.3
	T_L	Second		5.3 ± 0.2	4.45 ± 0.50	5.15 ± 0.20
0.20	$T_{\mathrm{HTI},1}$	Second	7.45 ± 0.20	6.9 ± 0.3	6.8 ± 0.3	6.7 ± 0.3
0.28	$T_{\mathrm{HTI},2}$	Second	5.65 ± 0.30	6.2 ± 0.3	6.3 ± 0.3	6.05 ± 0.30
0.35	$T_{\mathrm{HTI},2}$	Second	6.05 ± 0.30	6.35 ± 0.30	6.28 ± 0.30	6.35 ± 0.30
0.50	$T_{\mathrm{HTI},2}$	Second	7.45 ± 0.50	7.5 ± 0.3	7.5 ± 0.3	7.55 ± 0.30
	$T_{\mathrm{HTI},2}$	Second	9.42 ± 0.02	9.54 ± 0.05	9.52 ± 0.05	9.55 ± 0.10
	$T_{x,2}$	Second		7.13 ± 0.05	7.25 ± 0.05	7.16 ± 0.05
1	$T_{\mathrm{LTI},2}$	Second	6.48 ± 0.02	6.60 ± 0.04	6.50 ± 0.05	6.59 ± 0.05
($Ni_3V_2O_8$)	T_C	First	3.93 ± 0.02	3.93 ± 0.05	3.94 ± 0.05	3.90 ± 0.05
	$T_{C'}$	Second	2.42 ± 0.03	2.53 ± 0.05	2.50 ± 0.05	2.48 ± 0.05

$Ni_3V_2O_8$ are just the opposite as already visible in the mirrorlike temperature dependences of the expansivities. This is somewhat surprising since the incommensurate antiferromagnetic structure in $Co_3V_2O_8$ and $Ni_3V_2O_8$ have different propagation vectors and, even more, Co^{2+} and Ni^{2+} ions have different spin quantum numbers. Detailed calculations of the magnetic exchange interactions under uniaxial stress are needed to explain this. The thermal-expansion data suggest that uniaxial pressure is a very suitable tuning parameter to induce changes of the phase diagram. Applying uniaxial pressure along the c axis of $Co_3V_2O_8$ will lead to a suppression of all phase transitions, whereas in $Ni_3V_2O_8$, uniaxial pressure along the same direction is expected to enhance the transition temperatures. It would be particularly interesting to see if it is possible to suppress the magnetic order in $Co_3V_2O_8$ to zero temperature by uniaxial pressure along the c axis and then to see if a different type of magnetic order emerges at even higher pressures. Unfortunately, one would need about 5 GPa, which is experimentally extremely challenging. Closely related to the pressure dependences of the transition temperatures are the magnetic Grüneisen parameters, which, for $Co_3V_2O_8$ and $Ni_3V_2O_8$, exhibit a divergent-like behavior over a limited temperature interval. The Grüneisen parameters are strongly reduced in magnitude for the intermediate concentrations. A sign change of the Grüneisen parameters is observed for intermediate compositions near $x_c \simeq 0.25$, which might signal the proximity to a quantum phase transition arising from the doping-induced discontinuous change of magnetic propagation vector. The cascade of magnetic transitions in both $Co_3V_2O_8$ and $Ni_3V_2O_8$ is corroborated by the complex behavior of the magnetic Grüneisen parameters observed in this work, which underlines a quite complex ordering scenario.

ACKNOWLEDGMENT

We acknowledge G. Lawes, T. Lorenz, and M. Garst for useful discussions and G. Lawes for communicating the data prior to publication.

APPENDIX: FOCUS ON THE TRANSITIONS

Here, we show in detail how we have extracted all characteristic magnetic transition temperatures, as well as the steps ΔS, $\Delta L_i/L_i$, ΔC_p, and $\Delta\alpha_i$, at the second-order transitions of the $(Co_{1-x}Ni_x)_3V_2O_8$ samples studied in this work.

Figure 9 shows how the different first-order transition temperatures have been extracted for each S and L_i data curve, as well as the jumps ΔS and $\Delta L_i/L_i$ at the transitions. Figure 10 shows how the different second-order transition temperatures of each sample have been extracted from each of our C_p and α_i data curve, as well as the jumps ΔC_p and $\Delta\alpha_i$ at the transitions. Table IV presents the values of the different transition temperatures extracted here from each data curve (C_p, α_a, α_b, and α_c). In Table I, an average value (with an appropriate error bar) has been retained for each transition.

[1]E. E. Sauerbrei, R. Faggiani, and C. Calvo, Acta Crystallogr. Sect. B: Struct. Crystallogr. Cryst. Chem. **29**, 2304 (1973).

[2]N. Rogado, G. Lawes, D. A. Huse, A. P. Ramirez, and R. J. Cava, Solid State Commun. **124**, 229 (2002).

[3]Y. Chen, J. W. Lynn, Q. Huang, F. M. Woodward, T. Yildirim, G. Lawes, A. P. Ramirez, N. Rogado, R. J. Cava, A. Aharony, O. Entin-Wohlman, and A. B. Harris, Phys. Rev. B **74**, 014430 (2006).

[4]G. Lawes, M. Kenzelmann, N. Rogado, K. H. Kim, G. A. Jorge, R. J. Cava, A. Aharony, O. Entin-Wohlman, A. B. Harris, T. Yildirim, Q. Z. Huang, S. Park, C. Broholm, and A. P. Ramirez, Phys. Rev. Lett. **93**, 247201 (2004).

[5]G. Lawes, A. B. Harris, T. Kimura, N. Rogado, R. J. Cava, A. Aharony, O. Entin-Wohlman, T. Yildrim, M. Kenzelmann, C. Broholm, and A. P. Ramirez, Phys. Rev. Lett. **95**, 087205 (2005).

[6]Y. Yasui, Y. Kobayashi, M. Soda, T. Moyoshi, M. Sato, N. Igawa, and K. Kakurai, J. Phys. Soc. Jpn. **76**, 034706 (2007).

[7]N. Qureshi, H. Fuess, H. Ehrenberg, T. C. Hansen, C. Ritter, Th. Wolf, C. Meingast, Q. Zhang, W. Knafo, and H. von Löhneysen, J. Phys.: Condens. Matter **20**, 235228 (2008).

[8]N. Qureshi, H. Fuess, H. Ehrenberg, T. C. Hansen, C. Ritter, P. Adelmann, C. Meingast, Th. Wolf, Q. Zhang, and W. Knafo, J. Phys.: Condens. Matter **20**, 095219 (2008).

[9]Q. Zhang, W. Knafo, K. Grube, H. von Löhneysen, C. Meingast, and Th. Wolf, Phys. B **403**, 1404 (2008).

[10]N. R. Wilson, O. A. Petrenko, and G. Balakrishnan, J. Phys.: Condens. Matter **19**, 145257 (2007).

[11]R. P. Chaudhury, F. Yen, C. R. dela Cruz, B. Lorenz, Y. Q. Wang, Y. Y. Sun, and C. W. Chu, Phys. Rev. B **75**, 012407 (2007).

[12]Y. Kobayashi, Y. Yasui, and M. Sato, J. Magn. Magn. Mater. **310**, 1160 (2007).

[13]M. Garst and A. Rosch, Phys. Rev. B **72**, 205129 (2005).

[14]J. C. Lashley, M. F. Hundley, A. Migliori, J. L. Sarrao, P. G. Pagliuso, T. W. Darling, M. Jaime, J. C. Cooley, W. L. Hults, L. Morales, D. J. Thoma, J. L. Smith, J. Boerio-Goates, B. F. Woodfield, G. R. Stewart, R. A. Fisher, and N. E. Phillips, Cryogenics **43**, 369 (2003).

[15]H. Suzuki, A. Inaba, and C. Meingast, Cryogenics **50**, 693 (2010).

[16]C. Meingast, B. Blank, H. Bürkle, B. Obst, T. Wolf, H. Wühl, V. Selvamanickam, and K. Salama, Phys. Rev. B **41**, 11299 (1990).

[17]R. Pott and R. Schefzyk, J. Phys. E: Sci. Instrum. **16**, 444 (1983).

[18]Far below the magnetic ordering temperature, ungapped ferromagnetic spin waves are expected to lead to a T^d contribution to the specific heat, while ungapped antiferromagnetic spin waves are expected to lead to a $T^{d/2}$ contribution to the specific heat (d is the dimensionality of the magnetic system).

[19]M. Ramazanoglu, C. P. Adams, J. P. Clancy, A. J. Berlinsky, Z. Yamani, R. Szymczak, H. Szymczak, J. Fink-Finowicki, and B. D. Gaulin, Phys. Rev. B **79**, 024417 (2009).

[20]R. Szymczak, M. Baran, R. Diduszko, J. Fink-Finowicki, M. Gutowska, A. Szewczyk, and H. Szymczak, Phys. Rev. B **73**, 094425 (2006).

[21]R. Szymczak, P. Aleshkevych, C. P. Adams, S. N. Barilo, A. J. Berlinsky, J. P. Clancy, V. Domuchowski, J. Fink-Finowicki, B. D. Gaulin, M. Ramazanoglu, S. V. Shiryaev, Z. Yamani, and H. Szymczak, J. Magn. Magn. Mater. **321**, 793 (2009).

[22]Z. He, Y. Ueda, and M. Itoh, J. Cryst. Growth **297**, 1 (2006).

[23]M. E. Lines, Phys. Rev. **131**, 546 (1963).

[24]A. Kumarasiri and G. Lawes, Phys. Rev. B **84**, 064447 (2011).

[25]S. A. Grigera, R. A. Borzi, A. P. Mackenzie, S. R. Julian, R. S. Perry, and Y. Maeno, Phys. Rev. B **67**, 214427 (2003).

[26]J. Flouquet, *Progress in Low Temperature Physics* Vol. 15 (Elsevier, Amsterdam, 2005), Ch. 2, p. 139.

[27]H. von Löhneysen, A. Rosch, M. Vojta, and P. Wölfle, Rev. Mod. Phys. **79**, 1015 (2007).

[28]W. Knafo, S. Raymond, P. Lejay, and J. Flouquet, Nat. Phys. **5**, 753 (2009).

[29]O. Stockert, H. v. Löhneysen, A. Rosch, N. Pyka, and M. Loewenhaupt, Phys. Rev. Lett. **80**, 5627 (1998).

[30]S. Raymond, W. Knafo, J. Flouquet, F. Bourdarot, and P. Lejay, Phys. Status Solidi B **270**, 700 (2010).

[31]H. V. Löhneysen, M. Sieck, O. Stockert, and M. Waffenschmidt, Phys. B (Amsterdam) **223-224**, 471 (1996).

[32]C. Paulsen, A. Lacerda, L. Puech, P. Haen, P. Lejay, J. L. Tholence, J. Flouquet, and A. Visser, J. Low Temp. Phys. **81**, 317 (1990).

[33]S. Zaum, S. Drobnik, K. Grube, and H. V. Löhneysen (unpublished).

[34]W. Knafo, C. Meingast, A. V. Boris, P. Popovich, N. N. Kovaleva, P. Yordanov, A. Maljuk, R. K. Kremer, H. V. Löhneysen, and B. Keimer, Phys. Rev. B **79**, 054431 (2009).